

A genetic toolkit for studying transposon control in the *Drosophila melanogaster* ovary

Mostafa F. ElMaghraby,^{1,2,†} Laszlo Tirian,^{1,†} Kirsten-André Senti,¹ Katharina Meixner,¹ and Julius Brennecke ^{1,*}

¹Institute of Molecular Biotechnology of the Austrian Academy of Sciences (IMBA), Vienna BioCenter (VBC), Vienna 1030, Austria and

²Vienna BioCenter PhD Program, Doctoral School at the University of Vienna and Medical University of Vienna, Vienna 1030, Austria

[†]These authors contributed equally to this work.

*Corresponding author: Institute of Molecular Biotechnology of the Austrian Academy of Sciences, Vienna BioCenter, Dr. Bohr-Gasse 3, Vienna 1030, Austria.

Email: julius.brennecke@imba.oew.ac.at

Abstract

Argonaute proteins of the PIWI clade complexed with PIWI-interacting RNAs (piRNAs) protect the animal germline genome by silencing transposable elements. One of the leading experimental systems for studying piRNA biology is the *Drosophila melanogaster* ovary. In addition to classical mutagenesis, transgenic RNA interference (RNAi), which enables tissue-specific silencing of gene expression, plays a central role in piRNA research. Here, we establish a versatile toolkit focused on piRNA biology that combines germline transgenic RNAi, GFP marker lines for key proteins of the piRNA pathway, and reporter transgenes to establish genetic hierarchies. We compare constitutive, pan-germline RNAi with an equally potent transgenic RNAi system that is activated only after germ cell cyst formation. Stage-specific RNAi allows us to investigate the role of genes essential for germline cell survival, for example, nuclear RNA export or the SUMOylation pathway, in piRNA-dependent and independent transposon silencing. Our work forms the basis for an expandable genetic toolkit provided by the Vienna *Drosophila* Resource Center.

Keywords: *Drosophila*; oogenesis; germline; Gal4-UAS; piRNA pathway; transposable elements; RNAi; RNA export; SUMO

Introduction

Transposable elements (TEs) are mobile, selfish genetic elements that have parasitized almost all eukaryotic genomes and pose a threat to genome integrity (Feschotte 2008; Fedoroff 2012). In plants, fungi, and animals, small RNA silencing pathways are centrally involved in TE silencing, indicating an ancient function of RNA interference pathways in protecting the genome (Malone and Hannon 2009). In the animal germline, genome defense guided by small RNAs is carried out by Argonaute proteins of the PIWI-clade and their bound PIWI-interacting RNAs (piRNAs) (Siomi et al. 2011; Czech et al. 2018; Ozata et al. 2019). Most piRNAs originate from discrete genomic loci called piRNA clusters, which are rich in TE insertions (Aravin et al. 2007; Brennecke et al. 2007; Houwing et al. 2007). Therefore, piRNAs can guide PIWI proteins to complementary TE transcripts, allowing their selective silencing at the transcriptional (nuclear PIWIs) and post transcriptional (cytoplasmic PIWIs) levels. Defects in the piRNA pathway are compatible with overall animal development but result in uncontrolled TE activity in gonads, DNA damage, ectopic recombination and sterility. As stable cell lines derived from germline cells are rare, and as the piRNA pathway can differ in different cell types, the arms race between TEs and the piRNA pathway must be studied within the context of a developing organism.

Drosophila oogenesis is one of the leading model systems for piRNA research. Two main cell types make up the fly ovary: (1)

germline cells (germline stem cells, dividing cystoblast cells, nurse cells, and oocyte) and (2) somatic support cells that form the stem cell niche and surround, nourish, and protect the germline cells (Hudson and Cooley 2014). Both, germline and somatic cells of the ovary harbor a functional piRNA pathway. However, these pathways differ in several aspects. For example, germline cells express three PIWI clade Argonautes (nuclear Piwi, cytoplasmic Aubergine and Ago3), whereas somatic cells of the ovary express only nuclear Piwi (Malone et al. 2009). The identity and biology of the genomic piRNA source loci also differ in the two cell types. piRNA clusters in the ovarian soma resemble canonical RNA Polymerase II transcription units with defined promoter, transcription start site, and termination site (Lau et al. 2009; Malone et al. 2009; Goriaux et al. 2014; Mohn et al. 2014). Germline piRNA clusters are instead specified at the chromatin level by the action of Rhino, a member of the heterochromatin protein 1 (HP1) family that recruits germline-specific variants of core gene expression factors to enable enhancer-independent transcription on both DNA strands within heterochromatic loci (Klattenhoff et al. 2009; Mohn et al. 2014; Zhang et al. 2014; Andersen et al. 2017). The resulting piRNA precursors are suppressed in splicing and canonical 3' end formation and are exported via a dedicated, germline-specific RNA export route to the cytoplasmic, perinuclear piRNA processing sites known as Nuage (Chen et al. 2016; ElMaghraby et al. 2019; Kneuss et al. 2019).

Received: May 20, 2021. Accepted: September 19, 2021

© The Author(s) 2021. Published by Oxford University Press on behalf of Genetics Society of America.

This is an Open Access article distributed under the terms of the Creative Commons Attribution License (<https://creativecommons.org/licenses/by/4.0/>), which permits unrestricted reuse, distribution, and reproduction in any medium, provided the original work is properly cited.

Defects in the germline piRNA pathway result in uncontrolled TE transcription and transposition and lead to persistent activation of the DNA damage checkpoint. As a result, oocyte patterning pathways are disrupted, and eggs laid by piRNA pathway mutant flies have dorso-ventral polarity defects (Theurkauf et al. 2006; Klattenhoff et al. 2007; Senti et al. 2015; Durdevic et al. 2018; Wang et al. 2018). Based on this phenotype, classic genetic screens have uncovered several piRNA pathway genes (Schupbach and Roth 1994; Cook et al. 2004; Wehr et al. 2006; Chen et al. 2007; Pane et al. 2007; Zamparini et al. 2011). With the development of transgenic RNAi and the establishment of genome-wide *Drosophila* RNAi libraries (Dietzl et al. 2007; Haley et al. 2008; Ni et al. 2008, 2011), reverse genetic screens have systematically revealed piRNA pathway genes (Czech et al. 2013; Handler et al. 2013). Depending on the Gal4 driver used, these screens were specific to the somatic or germline piRNA pathway. Together, they identified ~40 genes with specific functions in the piRNA pathway.

Transgenic RNAi in the germline is based on germline-specific Gal4 driver lines that activate the expression of long or short RNA hairpin constructs targeting a gene of interest. The two most powerful transgenic RNAi setups for the germline are: (1) Combining the Maternal Triple Driver (MTD-Gal4; a combination of COG-Gal4 on the X-chromosome, NGT-Gal4 on the second, and *nanos*-Gal4 on the third chromosome) (Grieder et al. 2000) with transgenes harboring short hairpins (shRNA; microRNA mimics) under UAS-control (Valium20/22 backbones from the Harvard TRiP collection) (Haley et al. 2008; Ni et al. 2011). And (2), the combination of a dual *nanos*-Gal4 driver line (consisting of NGT-Gal4 and *nanos*-Gal4) that activates the expression of UAS-controlled long dsRNA hairpins from the Vienna RNAi collection alongside the RNAi-boosting protein Dcr-2 (Dietzl et al. 2007; Wang and Elgin 2011). Both approaches result in potent silencing of target gene expression throughout oogenesis, from primordial germ cells to germline stem cells, nurse cells, and mature oocytes.

While the pan-germline knockdown approaches have been instrumental for piRNA pathway research, they are not without limitations. For example, the piRNA pathway intersects with several general cellular processes such as SUMOylation, transcription, chromatin modification pathways, and RNA export. Genetic disruption of these processes often leads to cell-lethal or pleiotropic phenotypes resulting in atrophic ovaries lacking germline cells, precluding meaningful analyses. Previous studies have identified and characterized alternative Gal4 driver lines that activate Gal4 expression in the female germline upon cystoblast differentiation (late germarium stages onward), leaving germline stem cells unaffected (Staller et al. 2013). This allows genes with cell-essential functions to be studied as ovarian development proceeds to a sufficient extent.

Here, we first combine pan-oogenesis transgenic RNAi with marker lines expressing GFP-tagged piRNA pathway proteins that have diverse molecular functions and sub-cellular localizations. This toolkit provides a cell biology assay for studying gene function within the germline piRNA pathway. We then introduce and characterize TOSk-Gal4, a combination of *osk*-Gal4 and α Tub67C-Gal4, which causes strong Gal4 expression in the female germline immediately after germline cyst formation. TOSk-Gal4 is compatible with short and long hairpin RNAi libraries and allows efficient depletion of genes essential for cell survival without drastically affecting ovarian morphology and integrity. We combine TOSk-Gal4 with various genetic and molecular tools to study

the interface between piRNA pathway, RNA export, and protein SUMOylation.

Materials and methods

Fly husbandry

Flies were maintained at 25°C under light/dark cycles and 60% humidity. For ovary dissection, flies were kept in cages on apple juice plates with yeast paste for at least 5 days before dissection. All fly strains used and generated in this study are listed in [Supplementary Table S1](#) and available via the VDRC (<https://stockcenter.vdrc.at/control/main>).

Generation of transgenic fly strains

We generated fly strains harboring short hairpin RNA (shRNA) expression cassettes by cloning shRNA sequences into the Valium-20 vector (Ni et al. 2011) modified with a white selection marker. Tagged fly strains were generated via insertion of desired tag (here FLAG-V5-eGFP) sequences into Pacman clones containing the gene locus of interest (Venken et al. 2009) via bacterial recombineering (Ejsmont et al. 2011).

RNA fluorescent in situ hybridization (RNA-FISH)

Five to ten ovary pairs were fixed in IF Fixing Buffer (4% formaldehyde, 0.3% Triton X-100, 1x PBS) for 20 min at room temperature, washed three times for 10 min in PBX, and permeabilized in 70% ethanol at 4°C overnight. Permeabilized ovaries were rehydrated in RNA-FISH wash buffer [10% (v/w) formamide in 2x SSC] for 10 min. Ovaries were resuspended in 50 μ l hybridization buffer [10% (v/w) dextran sulfate, 10% (v/w) formamide in 2x SSC] supplemented with 0.5 μ l of 25 μ M RNA-FISH probe set solution (Stellaris; oligo sequences in [Supplementary Table S2](#)). Hybridization was performed at 37°C overnight with rotation. Next, ovaries were washed twice with RNA-FISH wash buffer for 30 min at 37°C, and twice with 2xSSC solution for 10 min at room temperature. To visualize DNA, DAPI (1:10,000 dilution) was included in the first 2xSSC wash. Ovaries were mounted in ~40 μ l Prolong Diamond mounting medium and imaged on a Zeiss LSM-880 confocal-microscope with AiryScan detector.

Immunofluorescence staining of ovaries

Five to ten ovary pairs were dissected into ice-cold PBS and fixed in IF Fixing Buffer (4% formaldehyde, 0.3% Triton X-100, 1x PBS) for 20 min at room temperature with rotation. Fixed ovaries were washed thrice with PBX (0.3% Triton X-100, 1x PBS), 10 min each wash, and incubated in BBX (0.1% BSA, 0.3% Triton X-100, 1x PBS) for 30 min for blocking. Primary antibodies diluted in BBX were added to ovaries and binding was performed at 4°C overnight. After three 10 min-washes in PBX, ovaries were incubated with secondary antibodies (1:1000 dilution in BBX) at 4°C overnight. Afterwards, the ovaries were washed 4 times with PBX, with the second wash done with DAPI (1:50,000 dilution). To visualize the nuclear envelope, Alexa Fluor 647-conjugated wheat germ agglutinin (1:200 dilution in PBX; Thermo Fisher Scientific) was added after DAPI staining for 20 min. Ovaries were finally mounted in ~40 μ l Prolong Diamond mounting medium and imaged on a Zeiss LSM-880 confocal-microscope with AiryScan detector. The resulting images were processed using Fiji/ImageJ (Schindelin et al. 2012). [Supplementary Table S3](#) lists antibodies used in this study.

Western blot analysis

Ten ovary pairs were dissected in ice-cold PBS and homogenized with a plastic pestle in RIPA lysis buffer (50 mM Tris-HCl pH 7.5, 150 mM NaCl, 1% Triton X-100, 0.5% Na-deoxycholate, 0.1% SDS, 0.5 mM EGTA, 1 mM EDTA) freshly supplemented with 1 mM Pefabloc, cOmplete Protease Inhibitor Cocktail (Roche), and 1 mM DTT. The samples were centrifuged at 14,000 rpm for 5 min, and the homogenization step was repeated. Samples were then incubated on ice for 30 min and cleared by centrifugation at 14,000 rpm for 15 min. Protein concentrations were quantified by Bradford reagent, and 10 µg total protein were resolved by SDS-polyacrylamide gel electrophoresis and transferred to a 0.2 µm nitrocellulose membrane (Bio-Rad). The membrane was blocked in 5% skimmed milk powder in PBX (0.01% Triton X-100 in PBS) and incubated with primary antibody overnight at 4°C (Supplementary Table S3). After three washes with PBX, the membrane was incubated with HRP-conjugated secondary antibody for 1 h at room temperature, followed by three washes with PBX. Subsequently, the membrane was covered with Clarity Western ECL Blotting Substrate (Bio-Rad) and imaged using the ChemiDoc MP imaging system (Bio-Rad).

RNA-Seq library preparation

Five ovary pairs were homogenized with a plastic pestle in 200 µl TRIzol reagent, and after homogenization 800 µl TRIzol were added and incubated for 5 min at room temperature. Two hundred microliter chloroform-isoamyl-alcohol (24:1; Sigma Aldrich) were added, and after vigorous shaking, samples were incubated for 5 min at room temperature. Next, samples were centrifuged at 12,000 g for 15 min at 4°C. RNA was extracted from the upper aqueous phase using the Direct-zol RNA Miniprep kit (Zymo Research) with on-column DNaseI treatment according to manufacturer's instructions. rRNA depletion from 1 µg total RNA was performed as described previously (ElMaghraby et al. 2019). Libraries were then cloned using the NEBNext Ultra II Directional RNA Library Prep Kit for Illumina (NEB), following the recommended kit protocol and sequenced on a NovaSeq 6000—SR100 (Illumina).

RT-qPCR analysis of transposon expression

Five pairs of dissected ovaries were homogenized in TRIzol reagent followed by RNA purification according to the manufacturer's protocol. One microgram of total RNA was reverse transcribed using the Maxima First Strand cDNA Synthesis kit (Thermo Fischer) following standard protocols. cDNA was used as template for RT-qPCR quantification of transposon mRNA levels (primer sequences in Supplementary Table S4).

Results and discussion

Combining pan-oogenesis RNAi with GFP-based piRNA pathway markers

Approximately forty proteins act in the *Drosophila* piRNA pathway (Czech et al. 2013; Handler et al. 2013). These factors serve different molecular functions and are localized to distinct subcellular locations in the nucleus (e.g., nucleoplasm or genomic piRNA source loci) and/or in the cytoplasm (e.g., outer mitochondrial membrane, perinuclear nuage). To visualize piRNA pathway proteins in whole mount ovary preparations by confocal microscopy, we generated transgenic fly lines carrying genomic rescue constructs with a FLAG-GFP tag at the N- or C-terminus of key piRNA pathway factors (four examples shown in Figure 1A). GFP-

tagging allows accurate and semi-quantitative determination of the subcellular localization of a protein as it circumvents the limitations of antigen accessibility to primary and secondary antibodies. This is particularly relevant in late-stage egg chambers (Figure 1B) or for factors enriched in peri-nuclear nuage such as Nxf3, Bootlegger, or Nibbler (Figure 1C).

To be able to analyze the subcellular localization of the different piRNA pathway proteins in flies with targeted genetic perturbations (using transgenic RNAi), we combined the established GFP marker lines with germline-specific Gal4 drivers. The resulting fly strains can be crossed with genome-wide collections of UAS lines that allow expression of long or short double-stranded RNA constructs targeting any gene of interest (available from Bloomington/TRiP or VDRC). Supplementary Figure S1 shows the crossing schemes underlying the construction of MTD-Gal4 lines [compatible with short hairpin RNA (shRNA) UAS-lines] or *nanos*-Gal4 lines with a UAS-Dcr-2 transgene (compatible with long hairpin RNA UAS-lines) harboring the various GFP reporter transgenes. Table 1 lists a core set of MTD-Gal4 lines combined to various GFP-markers that is available from the VDRC.

To illustrate the utility of the system, we focused on three subunits of the hexameric THO complex. THO is a key factor for nuclear mRNP quality control and, together with the RNA helicase UAP56 (Hel25E in *Drosophila*) and the adaptor protein Aly/Ref1, functions as a central gatekeeper for nuclear mRNP export (Heath et al. 2016). In germline cells, THO binds piRNA precursors derived from heterochromatic piRNA clusters in addition to mRNAs (Zhang et al. 2012; Hur et al. 2016; Zhang et al. 2018). Based on its central role in nuclear mRNA export, THO is also thought to be required for the export of piRNA precursors. Consistent with this, THO localizes broadly in the nucleoplasm in all cells, but is additionally enriched in germline cells at genomic piRNA source loci that are specified by the HP1 family protein Rhino (Hur et al. 2016; Zhang et al. 2018).

We generated MTD-Gal4 lines expressing GFP-tagged THO subunits Tho2, Thoc5, or Thoc7, and crossed them with UAS-shRNA lines targeting *rhino*, *thoc5*, or *thoc7* (a UAS-shRNA targeting *white* was used as a control throughout this study). As expected, depletion of Rhino resulted in loss of Tho2, Thoc5, and Thoc7 accumulation in discrete nuclear foci, confirming that THO localization to piRNA clusters depends on Rhino (Figure 1D) (Hur et al. 2016; Zhang et al. 2018). Loss of Thoc5 or Thoc7 revealed a strict co-dependence between both proteins for their stability, while Tho2 levels were only moderately affected in ovaries lacking Thoc5 or Thoc7 (Figure 1, D and E). However, Tho2 localization to nuclear foci (piRNA clusters) strictly depended on Thoc5 and Thoc7 (Figure 1D). Consistent with a critical role of THO at piRNA clusters, flies lacking Thoc5 or Thoc7 in the germline, despite having morphologically normal ovaries, were sterile. Their sterility was presumably linked to defects in piRNA precursor export, supported by instability of Nxf3, the dedicated RNA export receptor for piRNA precursors (Figure 1F). In line with this, flies with strong hypomorphic *thoc5* or *thoc7* alleles are viable but show loss of piRNAs from Rhino-dependent clusters and are sterile (Hur et al. 2016; Zhang et al. 2018). In contrast, depletion of Tho2 resulted in rudimentary ovaries, suggesting that Tho2 is genetically more important for mRNA export than the Thoc5 and Thoc7 subunits. These results are of interest in light of structural and biochemical studies of the human THO-UAP56 complex: whereas Tho2 is part of the THO core assembly (alongside Hpr1 and Tex), Thoc5 and Thoc7 form an extended coiled coil that is responsible for dimerization of the hexameric THO complex (Pühringer et al. 2020). Our results illustrate that the combination

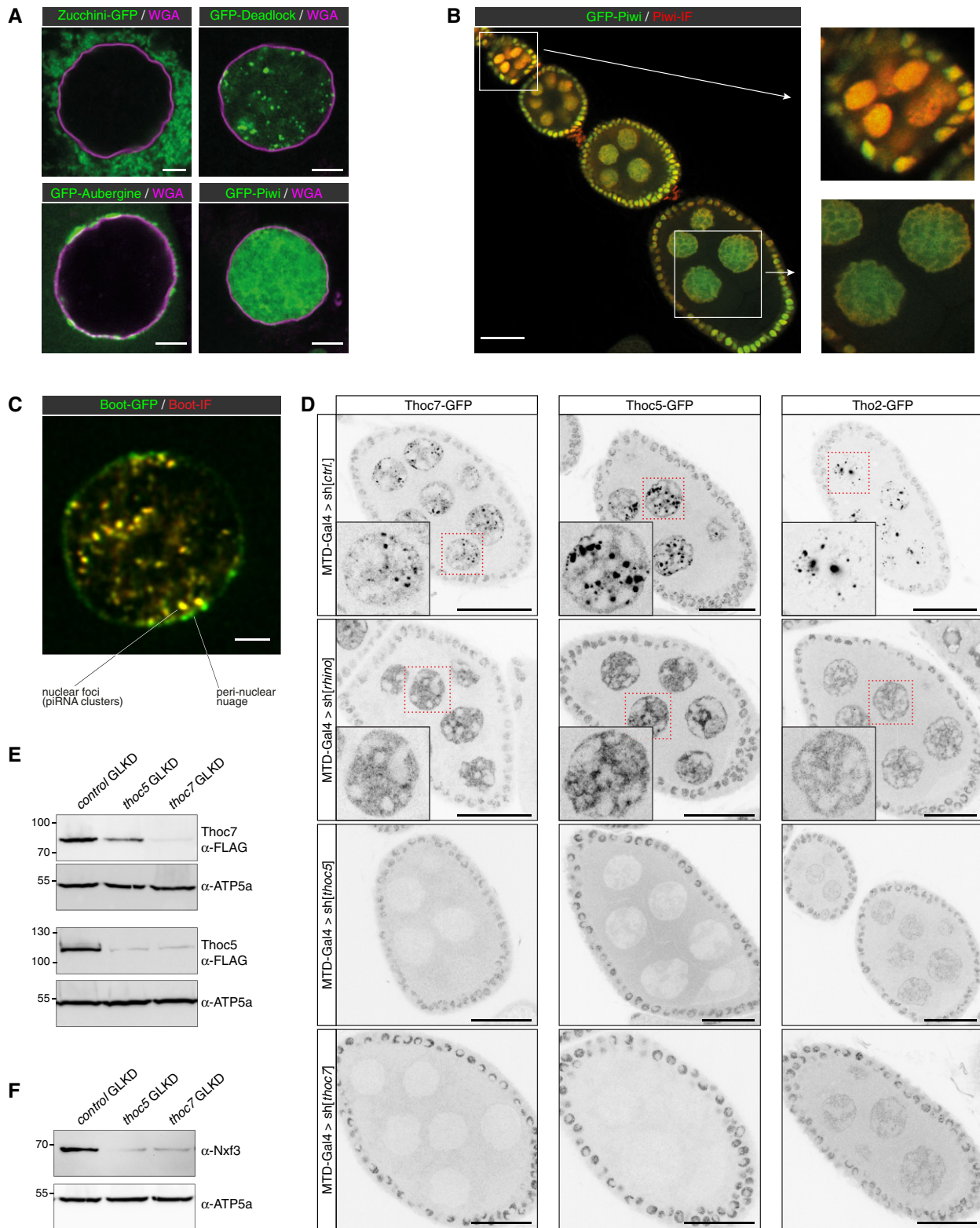


Figure 1 Pan-oogenesis RNAi with GFP-based piRNA pathway marker transgenes. (A) Confocal images (scale bars: 5 μ m) showing localization of GFP-tagged Zucchini (mitochondrial membrane), Deadlock (piRNA clusters), Aubergine (cytoplasm with nuage enrichment), and Piwi (nuclear) in germline nurse cell nuclei [nuclear envelope labeled with Wheat Germ Agglutinin (WGA), Alexa Fluor 647 in magenta]. (B) Confocal image (scale bar: 25 μ m) showing GFP-Piwi localization (green) in an ovariole stained also with anti-Piwi antibody (red). To the right, an enlarged early egg chamber with good overlap between GFP and immunofluorescence (IF) signals (top) and nurse cell nuclei from an older egg chamber where the GFP signal dominates due to reduced antibody penetration (bottom) are shown. (C) Confocal image (scale bar: 3 μ m) showing a nurse cell nucleus expressing Bootlegger-GFP (green) from the endogenous locus stained with an anti-Bootlegger antibody (red). Overlap between GFP and IF signals was apparent in nuclear foci, yet poor in nuage. (D) Confocal images of egg chambers (scale bars: 25 μ m) displaying localization of GFP-tagged Thoc7, Thoc5, or Tho2 (gray scale) in the indicated germline knockdown (GLKD) conditions (nuclei highlighted in red are enlarged). (E,F) Western blot analysis indicating levels of Thoc7 and Thoc5 (E), or Nxf3 (F) in ovary lysates from flies with indicated genotypes (anti ATP-synthase blots served as loading control).

Table 1 MTD-Gal4 reporter lines

	Name	Gene name	CG number	Source
THO/TREX	MTD-Gal4 + Thoc5-GFP	<i>thoc5</i>	CG2980	This work
	MTD-Gal4 + GFP-Thoc7	<i>thoc7</i>	CG17143	This work
	MTD-Gal4 + GFP-Tho2	<i>tho2</i>	CG31671	This work
piRNA cluster biology	MTD-Gal4 + GFP-Hel25E	<i>Hel25E</i>	CG7269	ElMaghraby et al. (2019)
	MTD-Gal4 + GFP-Rhino	<i>rhi</i>	CG10683	Mohn et al. (2014)
	MTD-Gal4 + GFP-Deadlock	<i>cuff</i>	CG13190	Mohn et al. (2014)
	MTD-Gal4 + GFP-Cutoff	<i>del</i>	CG9252	Mohn et al. (2014)
	MTD-Gal4 + GFP-Moonshiner	<i>moon</i>	CG12721	ElMaghraby et al. (2019)
	MTD-Gal4 + Nxf3-GFP	<i>Nxf3</i>	CG32135	ElMaghraby et al. (2019)
piRNA biogenesis	MTD-Gal4 + Bootlegger-GFP	<i>boot</i>	CG13741	ElMaghraby et al. (2019)
	MTD-Gal4 + Zucchini-GFP	<i>zuc</i>	CG12314	Hayashi et al. (2016)
	MTD-Gal4 + GFP-Gasz	<i>Gasz</i>	CG2183	This work
	MTD-Gal4 + GFP-Vasa	<i>vas</i>	CG46283	This work
	MTD-Gal4 + Spindle-E-GFP	<i>spn-E</i>	CG3158	This work
	MTD-Gal4 + GFP-Aubergine	<i>aub</i>	CG6137	This work
piRNA-mediated silencing and heterochromatin	MTD-Gal4 + GFP-Nibbler	<i>Nbr</i>	CG9247	This work
	MTD-Gal4 + GFP-Nxf2	<i>nxf2</i>	CG4118	This work
	MTD-Gal4 + GFP-Asterix	<i>arx</i>	CG3893	This work
	MTD-Gal4 + GFP-Panoramix	<i>Panx</i>	CG9754	This work
	MTD-Gal4 + GFP-Piwi	<i>piwi</i>	CG6122	This work
	MTD-Gal4 + Sov-GFPv	<i>sov</i>	CG14438	This work
	MTD-Gal4 + Su(var)3-9-GFP	<i>Su(var)3-9</i>	CG43664	This work
	MTD-Gal4 + GFP-Eggless	<i>egg</i>	CG12196	This work
	MTD-Gal4 + silencing reporter			Sienski et al. (2015)

of transgenic RNAi with GFP-transgenes is a powerful system to study protein function in the ovarian piRNA pathway and more generally during oogenesis.

A clear limitation of the pan-oogenesis Gal4 driver system is that genes, whose depletion is incompatible with oogenesis (*e.g.*, *tho2*), cannot be studied. Transgenic RNAi of genes with cell-essential functions results in rudimentary ovaries, often lacking detectable germline cells. Numerous genes (*e.g.*, those involved in heterochromatin establishment, SUMOylation, nuclear RNA export) that are required for a functional piRNA pathway can therefore not be studied in this manner. Inspired by previous studies (Staller et al. 2013; Yan et al. 2014), we set out to characterize alternative germline-specific Gal4 driver lines that, in combination with UAS-RNAi lines, are compatible with the analysis of cell-essential genes in the context of the ovarian piRNA pathway.

Efficient and specific transgenic RNAi in the differentiating female germline

Several germline-specific genes are transcribed in differentiating cysts but not during embryonic, larval, and pupal stages or in germline stem cells of the adult ovary. Gal4 driver lines exist for two of these genes: *oskar* (*osk*) and *alpha-Tubulin at 67C* (*αTub67C*) (Figure 2A) (Benton and St Johnston 2003; Telley et al. 2012). The *αTub67C*-Gal4 driver has been shown to induce efficient short-hairpin-based RNAi in ovaries (Staller et al. 2013; Yan et al. 2014). We set out to systematically compare *osk*-Gal4 and *αTub67C*-Gal4 to the pan-oogenesis MTD-Gal4. We first crossed each driver line with a fly line carrying a UASp-H2A-GFP transgene. In addition, we also induced H2A-GFP expression with *traffic jam* (*tj*)-Gal4, a somatic driver that is active in all somatic support cells of the ovary (Tanentzapf et al. 2007; Olivieri et al. 2010). Western blot analysis indicated that H2A-GFP levels in ovary lysate were comparable (*osk*-Gal4) to, or even higher (*αTub67C*-Gal4) than those from the MTD-Gal4 crosses (Figure 2B). However, in contrast to the MTD-Gal4 crosses, no H2A-GFP was detectable in germline stem cells and early germline cysts in the germarium for the *osk*-Gal4 or *αTub67C*-Gal4 crosses (Figure 2, A and C). We consistently observed that H2A-GFP expression initiated slightly earlier

(germarium region 2 b) for *osk*-Gal4 than for *αTub67C*-Gal4 (stage 2 egg chamber).

To evaluate the efficiency of the different drivers in inducing transgenic RNAi, we crossed them with flies carrying a very potent UAS-shRNA[GFP] transgene and one CRISPR-modified *piwi* allele harboring an N-terminal GFP-tag. As expected, MTD-Gal4 and *tj*-Gal4 induced strong depletion of GFP-Piwi in the entire ovarian germline or soma, respectively (Figure 2D). For *osk*-Gal4 and *αTub67C*-Gal4, GFP-Piwi levels were reduced from stage 2 egg chambers onwards and were undetectable in older egg chambers. As a more quantitative assay, we crossed the different Gal4 drivers with a UAS-shRNA[*piwi*] line and determined female sterility. shRNA-mediated depletion of Piwi with MTD-Gal4 resulted in 100% sterility (*n* = 200 laid eggs). For *osk*-Gal4 or *αTub67C*-Gal4, we observed near-complete sterility with occasional escapers (up to 3 escapers per 200 eggs laid). A driver line combining *αTub67C*-Gal4 and *osk*-Gal4 on the second chromosome, henceforth designated as *TOsk*-Gal4, resulted in complete sterility and was therefore used throughout this study.

We compared *TOsk*-Gal4 and MTD-Gal4 in the context of the germline piRNA pathway and depleted the two central Argonaute proteins Piwi or Aubergine (*Aub*) with UAS-shRNA lines. Endogenous Piwi or *Aub* proteins were undetectable in all germline cells for MTD-Gal4 and from stage 2/3 egg chambers onwards for *TOsk*-Gal4 (Figures 2E and 3A). For both Gal4 drivers, depletion of Piwi or *Aub* resulted in complete female sterility. To compare how depletion of Piwi with MTD-Gal4 vs *TOsk*-Gal4 impacts TE silencing, the central function of the germline piRNA pathway in *Drosophila*, we conducted RNA-seq experiments and, for selected TEs, RNA fluorescent *in situ* hybridization (FISH) experiments on ovaries with the different knockdown conditions. Overall, the same TEs that were de-repressed in ovaries depleted for Piwi during the entirety of oogenesis (MTD-Gal4) were also de-repressed, albeit at lower levels, in ovaries where transgenic RNAi was effective only from stage 3 egg chambers onwards (*TOsk*-Gal4) (Figure 3B). Examples for TEs exhibiting similar de-repression behavior are *blood* or *HMS Beagle* (Figure 3C). Mid and late-stage egg chambers (where loss of Piwi is indistinguishable

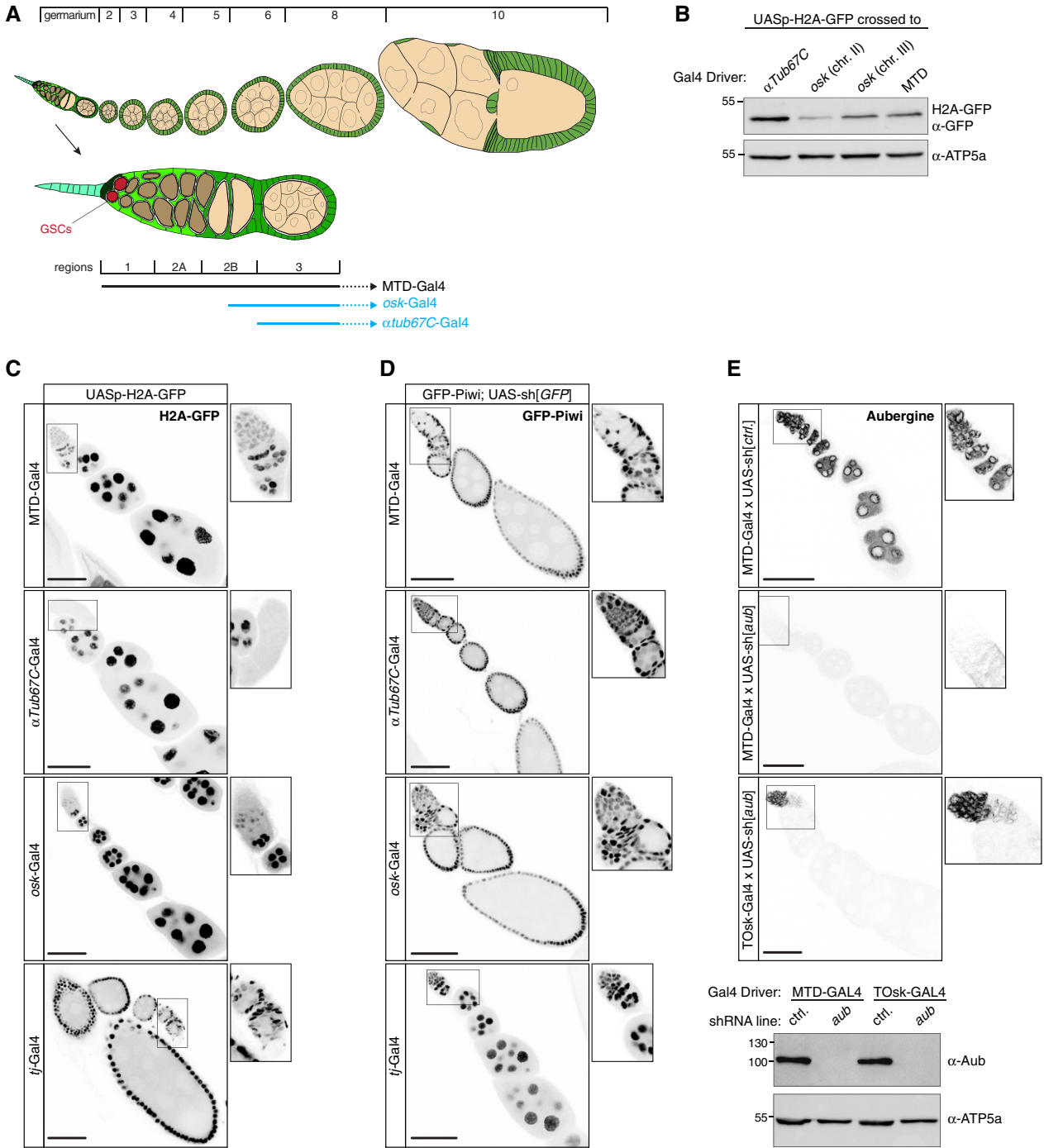


Figure 2 Efficient and specific transgenic RNAi in the differentiating female germline. (A) Cartoon of a *Drosophila* ovariole with somatic cells in green and germline cells in beige; egg chamber stages are indicated above and a magnified view of the germarium with stem cell niche is shown below. (B) Western blot analysis indicating levels of H2A-GFP expressed with indicated Gal4 drivers (anti ATP-synthase blot served as loading control). (C) Confocal images (scale bars: 50 μm) showing ovarioles expressing H2A-GFP (gray scale) driven by the indicated germline and soma Gal4 drivers (captions to the right show enlarged germaria). (D) Confocal images (scale bars: 50 μm) showing ovarioles expressing GFP-Piwi (gray scale) in the indicated genotypes (captions to the right show enlarged germaria). (E) Top: Confocal images (scale bars: 50 μm) showing ovarioles stained for Aubergine in the indicated genotypes (captions to the right show enlarged germaria). Bottom: Western blot analysis indicating levels of endogenous Aubergine in ovarian lysates from flies with the indicated genotypes (anti ATP-synthase blot served as loading control).

in MTD- vs TOsk-Gal4 crosses) contribute the bulk of the ovary mass and RNA. We therefore argue that the milder TE de-repression in the TOsk-Gal4 crosses is not due to differences in knockdown efficiency, but rather due to delayed TE de-silencing upon loss of piRNA pathway activity. Piwi-mediated

heterochromatin formation at TE loci likely contributes to this pattern. In agreement with this, steady-state RNA levels for the LTR retrotransposon *mdg3*, which is primarily repressed via Piwi-mediated heterochromatin formation (Senti et al. 2015) and whose steady-state RNA levels were more than 350-fold elevated

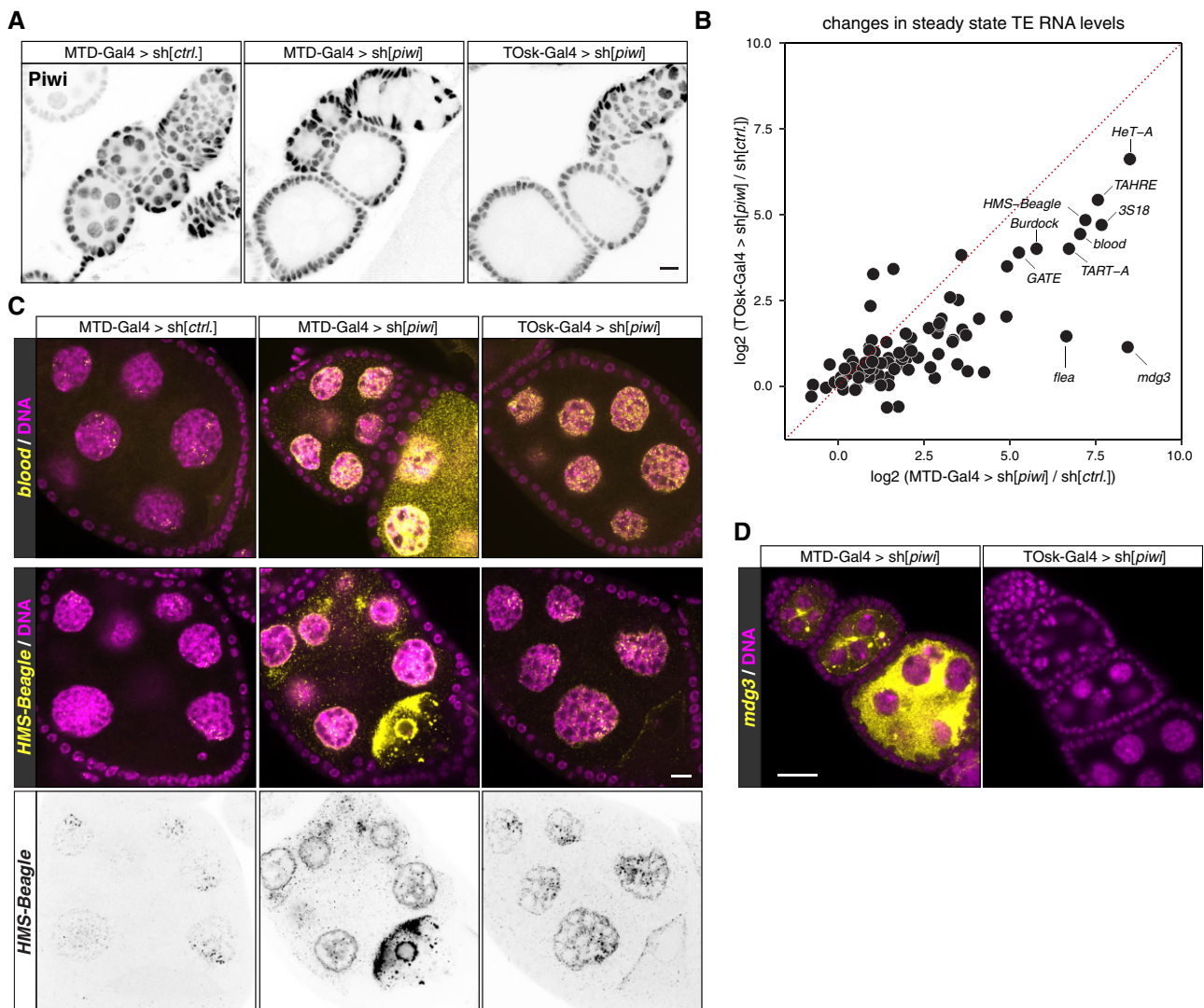


Figure 3 Comparison of MTD-Gal4 and Tosk-Gal4 driven transgenic RNAi. (A) Confocal images (scale bar: 10 μ m) showing ovarioles stained with anti-Piwi antibody (gray scale) in the indicated genotypes. (B) Scatter plot showing log₂ fold changes (relative to control) of TE steady-state RNA levels in ovaries where germline Piwi was depleted using MTD-Gal4 or Tosk-Gal4. (C and D) Confocal images (scale bars: 10 μ m) of egg chambers with indicated genotype stained for the TEs *blood* or *HMS-Beagle* (C), or for *mdg3* (D) using RNA-FISH (yellow; DAPI: magenta). The inverted black/white panels in (C) display the *HMS-Beagle* FISH signal alone (the nuclear signal in the control egg chamber is most likely signal from piRNA source loci).

upon MTD-Gal4-mediated Piwi knockdown, did not change more than \sim 2-fold when Piwi was depleted with Tosk-Gal4 (Figure 3, B and D). Taken together, Tosk-Gal4 allows very potent transgenic RNAi in germline cells of maturing egg chambers. In the case of the piRNA pathway, this results in a temporal delay in TE depression compared to a pan-germline knockdown.

Intersection points between piRNA pathway and essential cellular processes

To evaluate the utility of the Tosk-Gal4 transgenic RNAi system, we investigated biological processes that are required for transposon silencing and for cellular viability. We focused on the nuclear RNA export factors UAP56/Hel25E and Nxf1 (*Drosophila* Small bristles; Sbr), the protein exporter Crm1 (*Drosophila* Embargoed; Emb) (Zhang et al. 2012; ElMaghraby et al. 2019; Kneuss et al. 2019), and on the protein SUMOylation machinery with the E1 activating enzyme Uba2-Aos1 and the E3 Ligase Su(var)2-10 (Ninova et al. 2020). Depletion of any of these factors with MTD-Gal4 resulted in rudimentary ovaries, precluding any meaningful analysis as these lacked germline tissue, evidenced

by the absence of Aub expressing cells (Figures 4 and 5A; shown for Hel25E, Sbr). Crossing the same set of UAS-shRNA lines with the Tosk-Gal4 driver yielded flies with partially restored ovarian morphology and germline development.

Nuclear export of mRNA and piRNA precursors, both transcribed by RNA Polymerase II, requires the THO complex and the RNA Helicase Hel25E (Zhang et al. 2012, 2018; Hur et al. 2016; ElMaghraby et al. 2019). Together, these proteins license the loading of the RNA cargo onto a specific nuclear export receptor belonging to the NXF protein family (Sbr for mRNA, Nxf3 for piRNA precursors), which subsequently shuttles its respective RNA cargo through nuclear pore complexes into the cytoplasm (Kohler and Hurt 2007; ElMaghraby et al. 2019; Kneuss et al. 2019). Consistent with their central role in nuclear mRNA export, RNAi-mediated depletion of Sbr or Hel25E with MTD-Gal4 resulted in ovaries lacking germline cells (absence of Aub expressing cells; Figure 5A). Depletion of Hel25E or Sbr with Tosk-Gal4 also yielded sterile females. These flies, however, contained larger ovaries with clearly developing egg chambers, hence permitting molecular analyses (Figures 4 and 5A). We performed RNA-seq

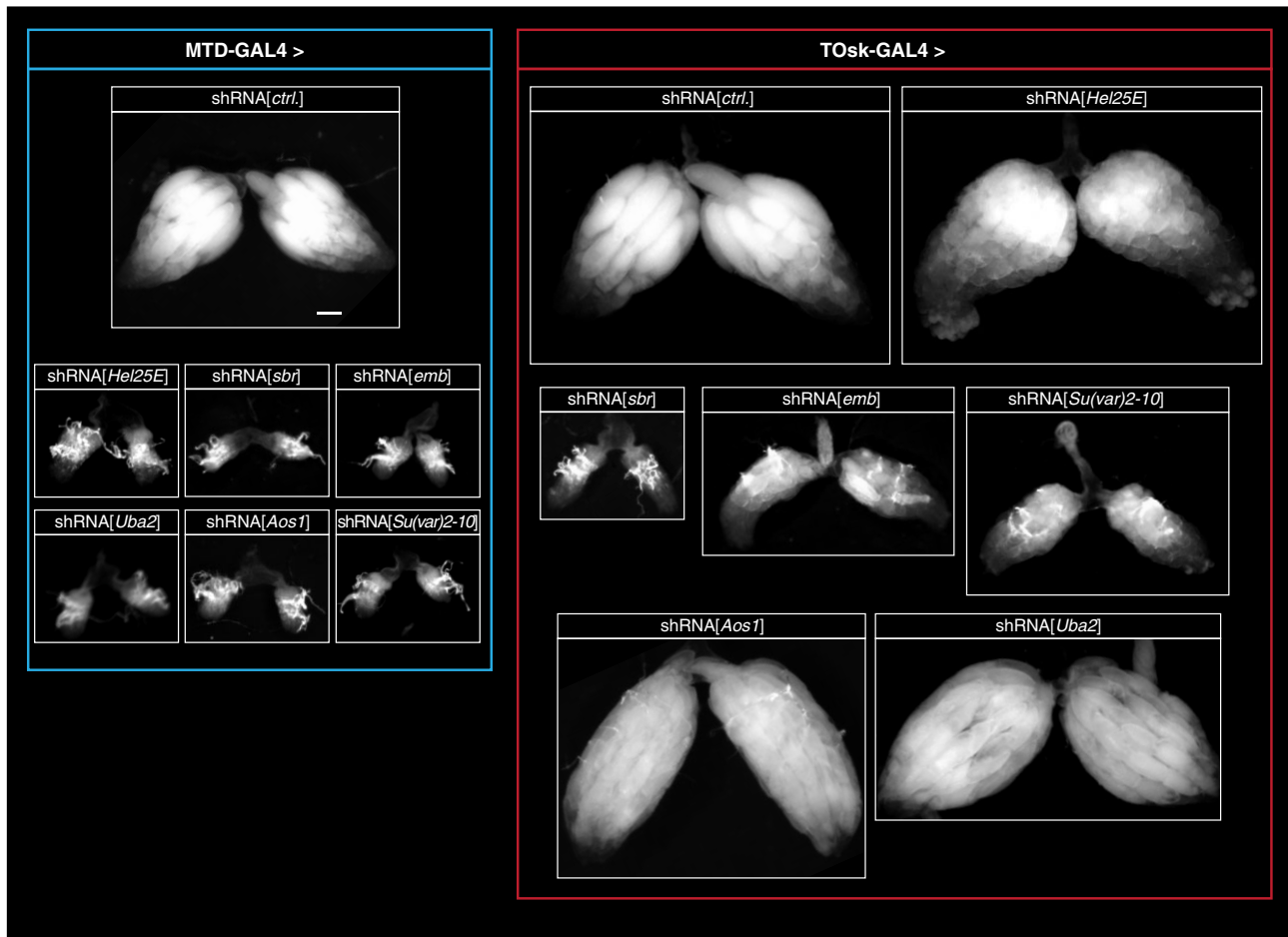


Figure 4 Transgenic RNAi of essential genes with TOSk-Gal4. Bright-field images (scale bar for all images: 200 μ m) showing ovarian morphology from flies of the indicated genotype (to the left: MTD-Gal4 crosses; to the right: TOSk-Gal4 crosses).

experiments on ovaries where Hel25E was depleted with TOSk-Gal4. Besides many genes that were de-regulated compared to control ovaries, numerous piRNA pathway repressed TEs were de-silenced (Figure 5B). In contrast, TE transcript levels were only mildly elevated in ovaries depleted of the essential mRNA export receptor Sbr (Figure 5C). An analysis on the LTR retroelement *blood* further showed that *blood* was not de-repressed in Sbr-depleted germline cells (Figure 5D). Instead, the increased *blood* transcript levels was due to expression in somatic cells and the fact that somatic cells contribute relatively more tissue in the Sbr-depleted ovaries compared to control ovaries. These findings support a direct role for Hel25E in the germline piRNA pathway that goes beyond nuclear export of mRNAs encoding for piRNA pathway proteins. Hel25E has therefore a dual role as a central gate keeper to feed RNA cargo into two distinct nuclear export receptors, Sbr-Nxt1 for mRNAs and Nxf3-Nxt1 for Rhino dependent piRNA precursors.

As a second intersection point between piRNA pathway and essential cellular processes, we chose piRNA-guided heterochromatin formation. The nuclear Argonaute protein Piwi, guided by its bound piRNAs, induces transcriptional gene silencing and specifies the local formation of heterochromatin at genomic TE insertions (Wang and Elgin 2011; Sienski et al. 2012; Le Thomas et al. 2013; Rozhkov et al. 2013). This process depends on transcription of a piRNA-complementary nascent transcript. To mediate silencing, piRNA-loaded Piwi requires a handful of piRNA pathway-specific factors (Gtsf1/Asterix, Maelstrom, SfiNX

complex) as well as factors of the general heterochromatin machinery that the piRNA pathway taps into (Czech et al. 2018; Ninova et al. 2019). Depletion of these general factors via MTD-Gal4 driven transgenic RNAi yields rudimentary ovaries with absent germline tissue. To explore the utility of the TOSk-Gal4 system, we focused on the protein SUMOylation pathway that is involved in numerous chromatin-related processes and that is required for Piwi-mediated transcriptional silencing and heterochromatin formation (Gareau and Lima 2010; Jentsch and Psakhye 2013; Ninova et al. 2020).

Protein SUMOylation requires E1 and E2 enzymes. *Drosophila* expresses a single E1 enzyme (Aos1-Uba2) and a single E2 enzyme (Lwr), which in a stepwise manner transfer a SUMO moiety onto a target lysine of the substrate. A handful of E3 ligases potentiate the SUMOylation process in a substrate-specific manner. Recent work has uncovered a critical role for the E3 ligase Su(var)2-10, and hence SUMOylation, in Piwi-mediated heterochromatin formation (Ninova et al. 2020). Depletion of Uba2, Aos1, or Su(var)2-10 with MTD-Gal4 was incompatible with GSC survival and oogenesis (Figure 4) (Yan et al. 2014). We therefore used TOSk-Gal4 driven transgenic RNAi to probe for a requirement for SUMOylation in the piRNA pathway. Piwi-mediated transcriptional silencing and heterochromatin formation can be mimicked by experimental tethering of the SfiNX complex to a nascent transcript using the λ N-boxB system (Figure 6A) (Sienski et al. 2015; Yu et al. 2015). In ovaries from flies that ubiquitously express a GFP reporter with boxB sites and that harbor the TOSk-Gal4 driver and a UASp- λ N-Panoramix (SfiNX

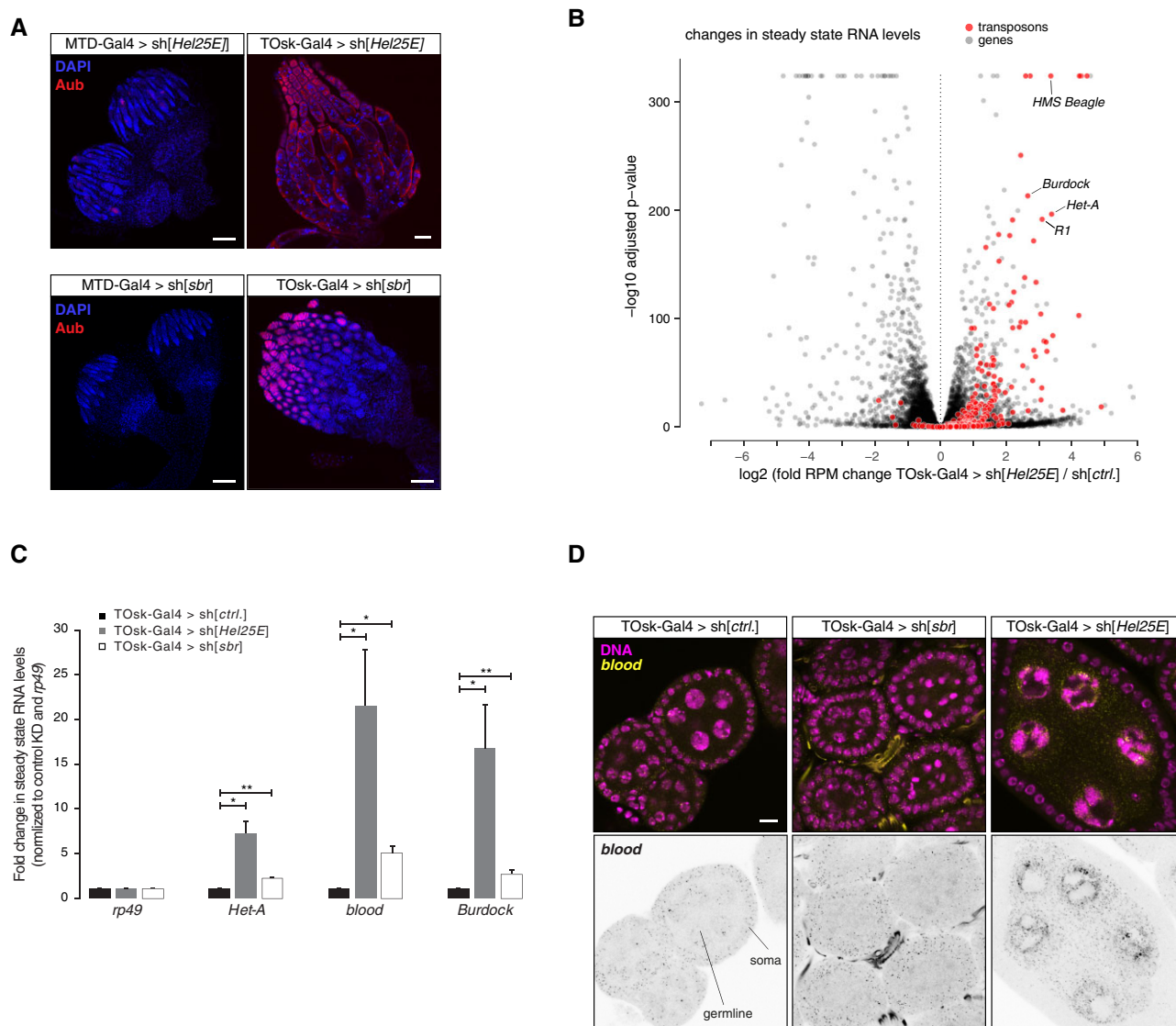


Figure 5 Dual role of Hel25E in mRNA export and transposon defense. (A) Confocal images (scale bars: 100 μ m) showing whole ovaries from flies of indicated genotypes stained with anti-Aubergine antibody (red); DNA stained with DAPI (blue). (B) Volcano plot showing fold changes in steady-state mRNA (black dots) and TE transcript levels (red dots) in ovaries from TOSk-Gal4 > sh[Hel25E] flies versus control flies ($n = 2$ biological replicates). (C) qRT-PCR analysis showing fold changes in steady-state TE transcript levels normalized to *rp49* mRNA levels in ovaries from flies with indicated genotypes ($n = 3$ biological replicates; * $P < 0.05$; ** $P < 0.01$ based on unpaired t-test). (D) Confocal images (scale bars: 10 μ m) of egg chambers with indicated genotype stained for the TEs *blood* using RNA-FISH (yellow; DAPI: magenta). The inverted black/white panels below show the *blood* FISH signal alone (tubular structures in the RNA-FISH channel stems from auto-fluorescence of trachea).

subunit) construct, GFP expression was silenced specifically in the germline from stage 3 egg chambers onwards (Figure 6B). Simultaneous expression of shRNA constructs targeting Piwi, which acts upstream of SFiNX, had no impact on GFP silencing. Similarly, targeting the mRNA exporter Sbr (Nxf1) did not interfere with SFiNX function, supporting the specificity of the assay. In contrast, depletion of the SUMOylation machinery [Aos1, Uba2, or Su(var)2-10] restored GFP expression confirming that protein SUMOylation is required for SFiNX-mediated heterochromatin formation (Figure 6B).

To obtain a more quantitative and systematic impact of the SUMOylation pathway on TE silencing in the female germline, we performed RNA-seq experiments on ovaries depleted (via TOSk-Gal4) for Piwi, Uba2, Aos1, or Su(var)2-10 and compared TE transcript levels to those in control ovaries. Depletion of Piwi or Su(var)2-10 resulted in overall similar TE silencing defects

(Figure 6C). When comparing TE transcript levels in Piwi depleted ovaries to those in ovaries depleted for the SUMO E1-ligase subunits Aos1 or Uba2, a similar set of TEs showed increased expression (Figure 6D). However, the R1 and R2 retrotransposons, two LINE elements that integrate specifically into rDNA units, were strong outliers as they showed nearly exclusive de-repression in ovaries lacking Aos1 or Uba2. In Aos1 or Uba2 depleted ovaries, steady-state RNA levels of R1 and R2 reached enormous levels and were among the most abundant cellular transcripts (Figure 6, D and E). R1 or R2 showed no de-repression in ovaries lacking Piwi (even when depleted via the MTD-Gal4 driver) although germline Piwi is loaded with R1 and R2 derived piRNAs. In agreement with a recent report (Luo et al. 2020), our data indicate that the SUMOylation pathway is integral for silencing R1 and R2, likely in a piRNA-independent and to a large extent also in a Su(var)2-10 independent manner.

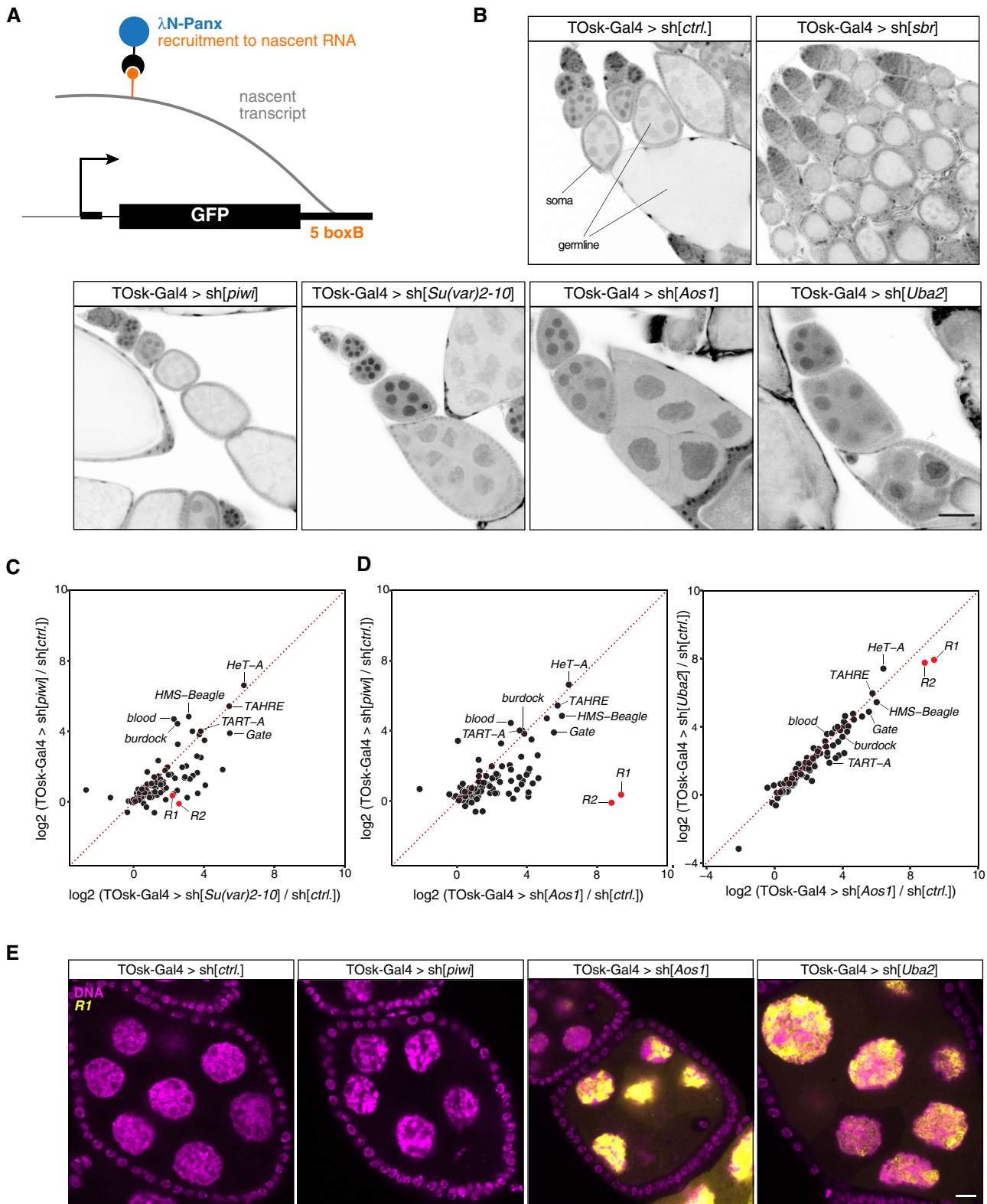


Figure 6 The SUMO machinery is required for TE repression in the germline. (A) Cartoon depicting the transgenic RNA-tethering reporter based on the λ N-boxB system. The α -tubulin promoter expresses GFP in all cells, and the 3' UTR harbors five boxB sites to allow tethering of λ N-Panx to the reporter mRNA. (B) Confocal images (scale bar: 50 μ m) showing GFP signal (gray scale) in egg chambers expressing the GFP-boxB reporter plus λ N-Panx and the indicated shRNAs specifically in the germline using TOsk-Gal4 (somatic cells serve as control). (C,D) Scatter plots based on RNA-seq data showing \log_2 fold changes (relative to control) in TE steady-state transcript levels in ovaries from flies of the indicated genotype. (E) Confocal images (scale bar: 10 μ m) of egg chambers from flies with indicated genotype showing R1 transposon mRNA using RNA-FISH (yellow; DAPI: magenta).

A TOsk-Gal4 system for long dsRNA hairpins and earlier expression

During our studies on the transgenic RNAi system using TOsk-Gal4, we encountered two technical aspects that warranted further modifications. While TOsk-Gal4 was highly efficient in depleting target genes using shRNA lines (e.g., TRIP collection), it was very inefficient with long dsRNA hairpin lines (VDRC collection). For example, when we crossed TOsk-Gal4 to UAS lines harboring long dsRNA hairpins targeting the SUMO-pathway, the resulting females were fertile, in stark contrast to crosses to shRNA lines targeting the same genes. This was reminiscent of the pan-oogenesis Gal4 driver system where efficient transgenic RNAi using long hairpin constructs requires the co-expression of the siRNA generating ribonuclease Dcr-2 (Wang and Elgin 2011). Indeed, when we combined TOsk-Gal4 with an X-chromosomal UAS-Dcr-2 transgene, knockdown of *Smt3* (*Drosophila* SUMO) as well as of the single E2 SUMO-conjugating enzyme *Lwr* yielded sterile females. These exhibited severe reductions in *Smt3* levels specifically in the germline (for the *smt3* knockdown) and the

characteristic strong de-repression of the R1 and R2 elements (Figure 7, A and B). Given the almost genome-wide collection of dsRNA hairpin lines at the VDRC, the TOsk-Gal4 > UAS-Dcr-2 combination stock will enable systematic genetic screens targeting genes that with a pan-oogenesis knockdown would yield rudimentary ovaries, often lacking germline tissue. We note that overexpression of Dcr-2 with TOsk-Gal4 results in female sterility. Therefore, virgins from VDRC RNAi lines must be crossed to males carrying TOsk-Gal4 and UAS-Dcr-2.

We finally considered the timing of oogenesis in respect to the onset of transgenic RNAi. The developmental process from germline stem cell division to mature egg takes nearly 1 week (Home-Badovinac and Bilder 2005; He et al. 2011). Up to 4 days are spent during the germarium stages, meaning before the onset of measurable depletion of target proteins using TOsk-Gal4. Though extraordinary efficient in depleting even abundant factors like Piwi or *Smt3*, this means that the time window of efficient transgenic RNAi is around 2–3 days. To extend this effective knockdown period, we turned to the *bam*-Gal4 driver,

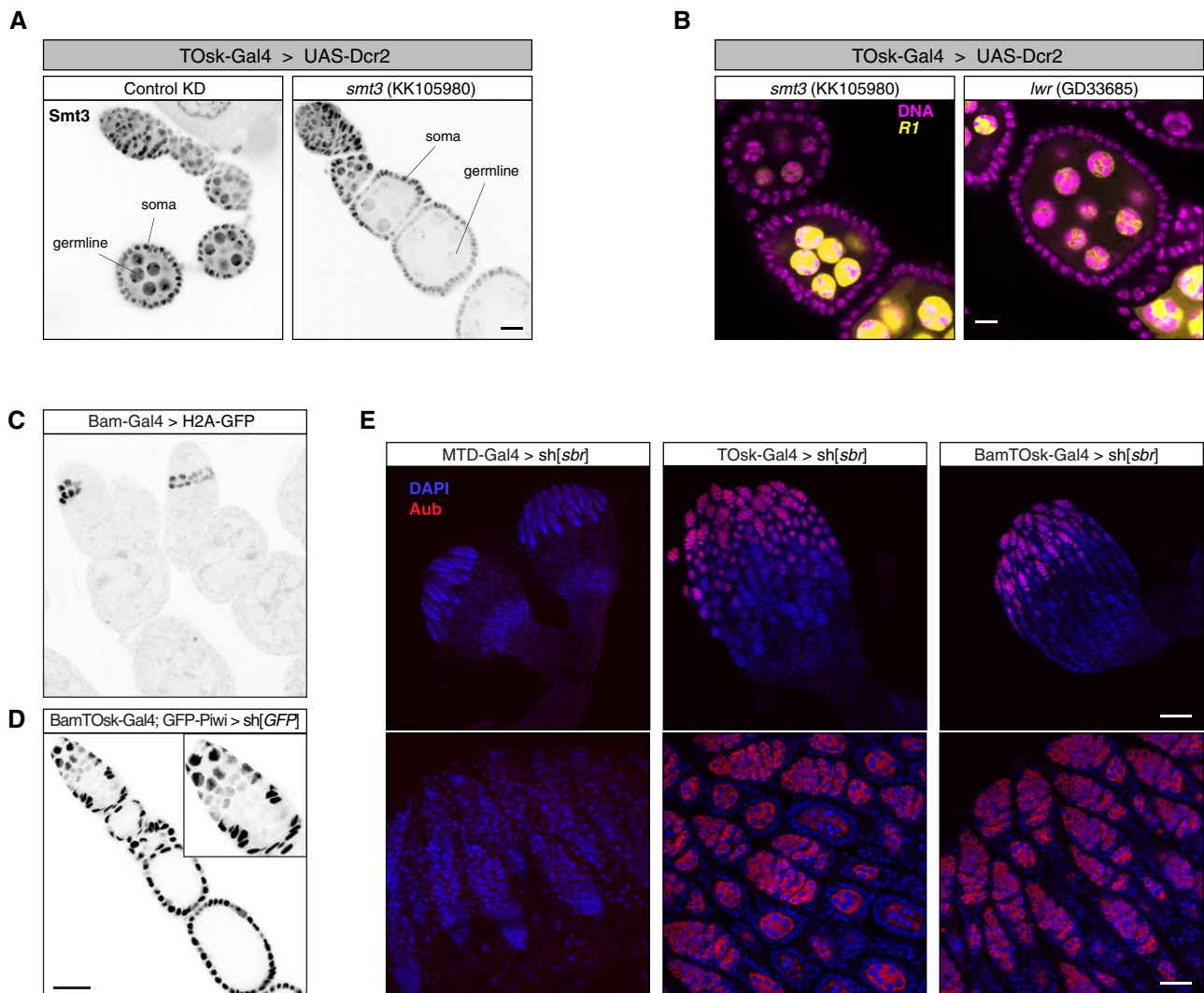


Figure 7 Extensions of the TOsk-Gal4 system. (A) Confocal images (scale bar: 10 μ m) showing ovarioles from flies with indicated genotype stained with anti-Smt3 antibody (gray scale). (B) Confocal images (scale bar: 10 μ m) of egg chambers from flies with indicated genotype showing R1 transcripts (RNA-FISH: yellow, DAPI: magenta). (C) Confocal image showing ovarioles expressing H2A-GFP driven by the *bam*-Gal4 driver. (D) Confocal image (scale bar: 25 μ m) showing GFP-Piwi levels (gray scale) in an ovariole expressing an sh[GFP] transgene with BamTOsk-Gal4 (inset shows the enlarged germarium; somatic cells serve as internal control). (E) Confocal images showing whole ovaries (top row; scale bar: 100 μ m) from flies of indicated genotype stained with anti-Aubergine antibody (red); DNA stained with DAPI (blue). Early oogenesis regions are highlighted in the bottom row (scale bar: 25 μ m).

which is expressed during a narrow time window of around one day at the onset of cystoblast division (Figure 7C) (Chen and McKearin 2003). When combining *bam*-Gal4 with TOsk-Gal4 (BamTOsk-Gal4), the knockdown of GFP-Piwi with an shRNA line against *GFP* indicated severe loss of Piwi already at the germlarium stage 2b, thereby extending the knockdown window of this triple driver to three to four days (Figure 7D). For a direct comparison of the various Gal4 driver combinations, we used the *sh[sbr]* line that leads to a highly potent depletion of the cell-essential mRNA export receptor *Sbr* (Figure 7E). Depletion of *Sbr* with the pan-oogenesis MTD-Gal4 driver resulted in the complete absence of germline tissue (no Aub positive cells). Depletion by TOsk-Gal4 resulted in phenotypically normal germlaria and two to four additional egg chambers per ovariole. The BamTOsk-Gal4 cross resulted in an intermediate phenotype with normal germlaria but only one additional egg chamber per ovariole. Thus, the BamTOsk-Gal4 driver represents an ideal driver to study gene function in the differentiating female germline via transgenic RNAi.

Taken all together, our work provides a versatile, highly specific and powerful genetic toolkit that permits tissue-specific RNAi at various stages of oogenesis in conjunction with GFP markers for the visualization of subcellular structures. While our focus was on piRNA biology, the presented approach is applicable to any expressed gene in the ovarian germline and complements previously established assays based on MTD-Gal4 or a double α Tub67C-Gal4 driver (Staller et al. 2013; Yan et al. 2014). Through the compatibility with genome-wide short and long UAS-dsRNA lines available from the Bloomington stock center or the VDRC, our work enables reverse genetic screens for the involvement of cell-essential factors in specific biological processes.

Data availability

Supplementary Table S1 lists all fly stocks used and generated in the study. All fly stocks are available via the Vienna *Drosophila* Resource Center or the Bloomington Stock Collection. Supplementary Table S2 lists Stellaris RNA-FISH probes used in this study. Supplementary Tables S3 and S4 list antibodies and oligo sequences used, respectively. Next-Generation Sequencing data produced in this publication have been deposited to the NCBI GEO archive under the accession number GSE174611. Supplementary Table S5 lists RNAseq libraries generated with respective SRA numbers, and sequencing and mapping quality statistics. The authors affirm that all data necessary for confirming the conclusions of the article are present within the article, figures, and tables.

Supplementary material is available at GENETICS online.

Acknowledgments

The authors thank D. Handler and M. Gehre for help with bioinformatics and computational analyses, the IMBA/IMP/GMI core facilities, in particular BioOptics for support, the Vienna Biocenter Core Facilities (VBCF) for providing NGS, COVID-19 testing, and fly stocks, and husbandry services (VDRC). Imre Gaspar and Daniel St. Johnston provided fly stocks. We sincerely thank Clemens Plaschka and Brennecke lab members for support and insightful discussions.

Funding

The Brennecke lab is supported by the Austrian Academy of Sciences, the European Research Council (ERC-2015-CoG - 682181), and the Austrian Science Fund (F4303 and W1207). M.F.E. is supported by a DOC Fellowship from the Austrian Academy of Sciences.

Author contributions

The project was conceived by J.B., M.F.E., and L.T. M.F.E. and L.T. performed all molecular biology and genetics experiments. K.A.S. conceptualized the BamTOsk-Gal4 driver and K.A.S. and K.M. generated essential reagents and fly stocks. J.B. supervised the study and M.F.E., L.T., and J.B. wrote the article with input from all authors.

Conflicts of interest

The authors declare that there is no conflict of interest.

Literature cited

- Andersen PR, Tirian L, Vunjak M, Brennecke J. 2017. A heterochromatin-dependent transcription machinery drives piRNA expression. *Nature*. 549:54–59.
- Aravin AA, Sachidanandam R, Girard A, Fejes-Toth K, Hannon GJ. 2007. Developmentally regulated piRNA clusters implicate MILL in transposon control. *Science*. 316:744–747.
- Benton R, St Johnston D. 2003. *Drosophila* PAR-1 and 14-3-3 inhibit Bazooka/PAR-3 to establish complementary cortical domains in polarized cells. *Cell*. 115:691–704.
- Brennecke J, Aravin AA, Stark A, Dus M, Kellis M, et al. 2007. Discrete small RNA-generating loci as master regulators of transposon activity in *Drosophila*. *Cell*. 128:1089–1103.
- Chen D, McKearin DM. 2003. A discrete transcriptional silencer in the *bam* gene determines asymmetric division of the *Drosophila* germline stem cell. *Development*. 130:1159–1170.
- Chen Y, Pane A, Schupbach T. 2007. Cutoff and aubergine mutations result in retrotransposon upregulation and checkpoint activation in *Drosophila*. *Curr Biol*. 17:637–642.
- Chen YA, Stuwe E, Luo Y, Ninova M, Thomas AL, et al. 2016. Cutoff suppresses RNA polymerase II termination to ensure expression of piRNA precursors. *Mol Cell*. 63:97–109.
- Cook HA, Koppetsch BS, Wu J, Theurkauf WE. 2004. The *Drosophila* SDE3 homolog Armitage is required for Oskar mRNA silencing and embryonic axis specification. *Cell*. 116:817–829.
- Czech B, Munafo M, Ciabrelli F, Eastwood EL, Fabry MH, et al. 2018. piRNA-guided genome defense: from biogenesis to silencing. *Annu Rev Genet*. 52:131–157.
- Czech B, Preall JB, McGinn J, Hannon GJ. 2013. A transcriptome-wide RNAi screen in the *Drosophila* ovary reveals factors of the germline piRNA pathway. *Mol Cell*. 50:749–761.
- Dietzl G, Chen D, Schnorrer F, Su KC, Barinova Y, et al. 2007. A genome-wide transgenic RNAi library for conditional gene inactivation in *Drosophila*. *Nature*. 448:151–156.
- Durdevic Z, Pillai RS, Ephrussi A. 2018. Transposon silencing in the *Drosophila* female germline is essential for genome stability in progeny embryos. *Life Sci Alliance*. 1:e201800179.
- Ejsmont RK, Bogdanzaliewa M, Lipinski KA, Tomancak P. 2011. Production of fosmid genomic libraries optimized for liquid culture recombineering and cross-species transgenesis. *Methods Mol Biol*. 772:423–443.

- ElMaghraby MF, Andersen PR, Puhlinger F, Hohmann U, Meixner K, et al. 2019. A heterochromatin-specific RNA export pathway facilitates piRNA production. *Cell*. 178:964–979.e920.
- Fedoroff NV. 2012. Presidential address. Transposable elements, epigenetics, and genome evolution. *Science*. 338:758–767.
- Feschotte C. 2008. Transposable elements and the evolution of regulatory networks. *Nat Rev Genet*. 9:397–405.
- Gareau JR, Lima CD. 2010. The SUMO pathway: emerging mechanisms that shape specificity, conjugation and recognition. *Nat Rev Mol Cell Biol*. 11:861–871.
- Goriaux C, Desset S, Renaud Y, Vaury C, Brassat E. 2014. Transcriptional properties and splicing of the flamenco piRNA cluster. *EMBO Rep*. 15:411–418.
- Grieder NC, de Cuevas M, Spradling AC. 2000. The fusome organizes the microtubule network during oocyte differentiation in *Drosophila*. *Development*. 127:4253–4264.
- Haley B, Hendrix D, Trang V, Levine M. 2008. A simplified miRNA-based gene silencing method for *Drosophila melanogaster*. *Dev Biol*. 321:482–490.
- Handler D, Meixner K, Pizka M, Lauss K, Schmied C, et al. 2013. The genetic makeup of the *Drosophila* piRNA pathway. *Mol Cell*. 50:762–777.
- Hayashi R, Schnabl J, Handler D, Mohn F, Ameres SL, et al. 2016. Genetic and mechanistic diversity of piRNA 3'-end formation. *Nature*. 539:588–592.
- He L, Wang X, Montell DJ. 2011. Shining light on *Drosophila* oogenesis: live imaging of egg development. *Curr Opin Genet Dev*. 21:612–619.
- Heath CG, Viphakone N, Wilson SA. 2016. The role of TREX in gene expression and disease. *Biochem J*. 473:2911–2935.
- Horne-Badovinac S, Bilder D. 2005. Mass transit: epithelial morphogenesis in the *Drosophila* egg chamber. *Dev Dyn*. 232:559–574.
- Houwing S, Kamminga LM, Berezikov E, Cronembold D, Girard A, et al. 2007. A role for Piwi and piRNAs in germ cell maintenance and transposon silencing in Zebrafish. *Cell*. 129:69–82.
- Hudson AM, Cooley L. 2014. Methods for studying oogenesis. *Methods*. 68:207–217.
- Hur JK, Luo Y, Moon S, Ninova M, Marinov GK, et al. 2016. Splicing-independent loading of TREX on nascent RNA is required for efficient expression of dual-strand piRNA clusters in *Drosophila*. *Genes Dev*. 30:840–855.
- Jentsch S, Psakhye I. 2013. Control of nuclear activities by substrate-selective and protein-group SUMOylation. *Annu Rev Genet*. 47:167–186.
- Klattenhoff C, Bratu DP, McGinnis-Schultz N, Koppetsch BS, Cook HA, et al. 2007. *Drosophila* rasiRNA pathway mutations disrupt embryonic axis specification through activation of an ATR/Chk2 DNA damage response. *Dev Cell*. 12:45–55.
- Klattenhoff C, Xi H, Li C, Lee S, Xu J, et al. 2009. The *Drosophila* HP1 homolog Rhino is required for transposon silencing and piRNA production by dual-strand clusters. *Cell*. 138:1137–1149.
- Kneuss E, Munafo M, Eastwood EL, Deumer US, Preall JB, et al. 2019. Specialization of the *Drosophila* nuclear export family protein Nxf3 for piRNA precursor export. *Genes Dev*. 33:1208–1220.
- Kohler A, Hurt E. 2007. Exporting RNA from the nucleus to the cytoplasm. *Nat Rev Mol Cell Biol*. 8:761–773.
- Lau NC, Robine N, Martin R, Chung WJ, Niki Y, et al. 2009. Abundant primary piRNAs, endo-siRNAs, and microRNAs in a *Drosophila* ovary cell line. *Genome Res*. 19:1776–1785.
- Le Thomas A, Rogers AK, Webster A, Marinov GK, Liao SE, et al. 2013. Piwi induces piRNA-guided transcriptional silencing and establishment of a repressive chromatin state. *Genes Dev*. 27:390–399.
- Luo Y, Fefelova E, Ninova M, Chen YA, Aravin AA. 2020. Repression of interrupted and intact rDNA by the SUMO pathway in *Drosophila melanogaster*. *Elife*. 9:e52416.
- Malone CD, Brennecke J, Dus M, Stark A, McCombie WR, et al. 2009. Specialized piRNA pathways act in germline and somatic tissues of the *Drosophila* ovary. *Cell*. 137:522–535.
- Malone CD, Hannon GJ. 2009. Small RNAs as guardians of the genome. *Cell*. 136:656–668.
- Mohn F, Sienski G, Handler D, Brennecke J. 2014. The rhino-deadlock-cutoff complex licenses noncanonical transcription of dual-strand piRNA clusters in *Drosophila*. *Cell*. 157:1364–1379.
- Ni JQ, Markstein M, Binari R, Pfeiffer B, Liu LP, et al. 2008. Vector and parameters for targeted transgenic RNA interference in *Drosophila melanogaster*. *Nat Methods*. 5:49–51.
- Ni JQ, Zhou R, Czech B, Liu LP, Holderbaum L, et al. 2011. A genome-scale shRNA resource for transgenic RNAi in *Drosophila*. *Nat Methods*. 8:405–407.
- Ninova M, Chen YA, Godneeva B, Rogers AK, Luo Y, et al. 2020. Su(var)2–10 and the SUMO pathway link piRNA-guided target recognition to chromatin silencing. *Mol Cell*. 77:556–570.e556.
- Ninova M, Fejes Toth K, Aravin AA. 2019. The control of gene expression and cell identity by H3K9 trimethylation. *Development*. 146:dev181180.
- Olivieri D, Sykora MM, Sachidanandam R, Mechtler K, Brennecke J. 2010. An in vivo RNAi assay identifies major genetic and cellular requirements for primary piRNA biogenesis in *Drosophila*. *EMBO J*. 29:3301–3317.
- Ozata DM, Gainetdinov I, Zoch A, O'Carroll D, Zamore PD. 2019. PIWI-interacting RNAs: small RNAs with big functions. *Nat Rev Genet*. 20:89–108.
- Pane A, Wehr K, Schupbach T. 2007. Zucchini and squash encode two putative nucleases required for rasiRNA production in the *Drosophila* germline. *Dev Cell*. 12:851–862.
- Pühlinger T, Hohmann U, Fin L, Pacheco-Fiallos B, Schellhaas U, et al. 2020. Structure of the human core transcription-export complex reveals a hub for multivalent interactions. *Elife*. 9:e61503.
- Rozhkov NV, Hammell M, Hannon GJ. 2013. Multiple roles for Piwi in silencing *Drosophila* transposons. *Genes Dev*. 27:400–412.
- Schindelin J, Arganda-Carreras I, Frise E, Kaynig V, Longair M, et al. 2012. Fiji: an open-source platform for biological-image analysis. *Nat Methods*. 9:676–682.
- Schupbach T, Roth S. 1994. Dorsoventral patterning in *Drosophila* oogenesis. *Curr Opin Genet Dev*. 4:502–507.
- Senti KA, Jurczak D, Sachidanandam R, Brennecke J. 2015. piRNA-guided slicing of transposon transcripts enforces their transcriptional silencing via specifying the nuclear piRNA repertoire. *Genes Dev*. 29:1747–1762.
- Sienski G, Batki J, Senti KA, Donertas D, Tirian L, et al. 2015. Silencio/CG9754 connects the Piwi-piRNA complex to the cellular heterochromatin machinery. *Genes Dev*. 29:2258–2271.
- Sienski G, Donertas D, Brennecke J. 2012. Transcriptional silencing of transposons by Piwi and maelstrom and its impact on chromatin state and gene expression. *Cell*. 151:964–980.
- Siomi MC, Sato K, Pezic D, Aravin AA. 2011. PIWI-interacting small RNAs: the vanguard of genome defence. *Nat Rev Mol Cell Biol*. 12:246–258.
- Staller MV, Yan D, Randklev S, Bragdon MD, Wunderlich ZB, et al. 2013. Depleting gene activities in early *Drosophila* embryos with the "maternal-Gal4-shRNA" system. *Genetics*. 193:51–61.
- Tanentzapf G, Devenport D, Godt D, Brown NH. 2007. Integrin-dependent anchoring of a stem-cell niche. *Nat Cell Biol*. 9:1413–1418.

- Telley IA, Gaspar I, Ephrussi A, Surrey T. 2012. Aster migration determines the length scale of nuclear separation in the *Drosophila* syncytial embryo. *J Cell Biol.* 197:887–895.
- Theurkauf WE, Klattenhoff C, Bratu DP, McGinnis-Schultz N, Koppetsch BS, et al. 2006. rasiRNAs, DNA damage, and embryonic axis specification. *Cold Spring Harb Symp Quant Biol.* 71:171–180.
- Venken KJ, Carlson JW, Schulze KL, Pan H, He Y, et al. 2009. Versatile P[acman] BAC libraries for transgenesis studies in *Drosophila melanogaster*. *Nat Methods.* 6:431–434.
- Wang L, Dou K, Moon S, Tan FJ, Zhang ZZ. 2018. Hijacking oogenesis enables massive propagation of LINE and retroviral transposons. *Cell.* 174:1082–1094.e1012.
- Wang SH, Elgin SC. 2011. *Drosophila* Piwi functions downstream of piRNA production mediating a chromatin-based transposon silencing mechanism in female germ line. *Proc Natl Acad Sci USA.* 108:21164–21169.
- Wehr K, Swan A, Schupbach T. 2006. Deadlock, a novel protein of *Drosophila*, is required for germline maintenance, fusome morphogenesis and axial patterning in oogenesis and associates with centrosomes in the early embryo. *Dev Biol.* 294:406–417.
- Yan D, Neumuller RA, Buckner M, Ayers K, Li H, et al. 2014. A regulatory network of *Drosophila* germline stem cell self-renewal. *Dev Cell.* 28:459–473.
- Yu Y, Gu J, Jin Y, Luo Y, Preall JB, et al. 2015. Panoramix enforces piRNA-dependent cotranscriptional silencing. *Science.* 350:339–342.
- Zamparini AL, Davis MY, Malone CD, Vieira E, Zavadil J, et al. 2011. Vreteno, a gonad-specific protein, is essential for germline development and primary piRNA biogenesis in *Drosophila*. *Development.* 138:4039–4050.
- Zhang F, Wang J, Xu J, Zhang Z, Koppetsch BS, et al. 2012. UAP56 couples piRNA clusters to the perinuclear transposon silencing machinery. *Cell.* 151:871–884.
- Zhang G, Tu S, Yu T, Zhang XO, Parhad SS, et al. 2018. Co-dependent assembly of *Drosophila* piRNA precursor complexes and piRNA cluster heterochromatin. *Cell Rep.* 24:3413–3422.e3414.
- Zhang Z, Wang J, Schultz N, Zhang F, Parhad SS, et al. 2014. The HP1 homolog rhino anchors a nuclear complex that suppresses piRNA precursor splicing. *Cell.* 157:1353–1363.

Communicating editor: J. Claycomb